Smart Structures and Systems, *Vol. 19, No. 2 (2017) 163-179*
DOI: https://doi.org/10.12989/sss.2017.19.2.163

Buckling delamination of the PZT/Metal/PZT sandwich circular plate-disc with penny-shaped interface cracks

Fazile I. Cafarova[1a], Surkay D. Akbarov[*2,3] and Nazmiye Yahnioglu[4b]

[1]*Genje State University, Genje, Azerbaijan*
[2]*Department of Mechanical Engineering, Yildiz Technical University 34349, Besiktas, Istanbul, Turkey*
[3]*Institute of mathematics and Mechanics of the National Academy of Sciences of Azerbaijan, AZ1141, Baku, Azerbaijan*
[4]*Department of Mathematical Engineering, Yildiz Technical University, Davutpasa Campus, 34220, Esenler, Istanbul, Turkey*

(Received April 6, 2016, Revised December 1, 2016, Accepted December 5, 2016)9pt

Abstract. The axisymmetric buckling delamination of the Piezoelectric/Metal/Piezoelectric (PZT/Metal/PZT) sandwich circular plate with interface penny-shaped cracks is investigated. The case is considered where open-circuit conditions with respect to the electrical displacement on the upper and lower surfaces, and short-circuit conditions with respect to the electrical potential on the lateral surface of the face layers are satisfied. It is assumed that the edge surfaces of the cracks have an infinitesimal rotationally symmetric initial imperfection and the development of this imperfection with rotationally symmetric compressive forces acting on the lateral surface of the plate is studied by employing the exact geometrically non-linear field equations and relations of electro-elasticity for piezoelectric materials. The sought values are presented in the power series form with respect to the small parameter which characterizes the degree of the initial imperfection. The zeroth and first approximations are used for investigation of stability loss and buckling delamination problems. It is established that the equations and relations related to the first approximation coincide with the corresponding ones of the three-dimensional linearized theory of stability of electro-elasticity for piezoelectric materials. The quantities related to the zeroth approximation are determined analytically, however the quantities related to the first approximation are determined numerically by employing Finite Element Method (FEM). Numerical results on the critical radial stresses acting in the layers of the plate are presented and discussed. In particular, it is established that the piezoelectricity of the face layer material causes an increase (a decrease) in the values of the critical compressive stress acting in the face (core) layer.

Keywords: piezoelectric material; circular sandwich plate; penny-shaped crack; buckling delamination; critical stress

1. Introduction

Piezoelectric thin samples are used as sensors and actuators for controlling the working procedures of various types of elements of construction such as plates and shells. Under agglutination, debonded zones can arise on these samples on the face surface of the elements of construction. Specifically, these debonded zones may be the source of local buckling of the piezoelectric samples under compressional electromechanical forces. Consequently, such situations prevent the piezoelectric sample-plates from performing properly as sensors and actuators. For controlling and preventing such buckling delamination it is necessary to make related theoretical investigations. However, up to recent years such investigations have been almost completely absent. However, the study of the stability loss problems of the piezoelectric plates and beams has attracted the attention of many researchers such as Yang (1998), Jerom and Ganesan (2010) and many others listed therein. In these investigations it was established that the piezoelectricity of the plate or beam materials causes an increase in the values of the mechanical critical forces. There are also a number investigations on the dynamics, statics and stability loss of the systems consisting of piezoelectric and elastic constituents. Some of them are briefly reviewed below.

The paper by Kakar and Kakar (2016) deals with the study of the Shear-Horizontal (SH)-waves in the system comprising a piezomagnetic covering layer and an initially stressed orthotropic half-plane. The corresponding dispersion equation is derived for both magnetically open- and closed- circuit cases under various types of boundary conditions on the free face plane of the piezomagnetic layer. Numerical results illustrating the influence of the piezomagnetic properties of the covering layer on the dispersion curves are presented and discussed.

In the paper by Wu and Ding (2015), static analysis of the simply supported rectangular plate made of functionally graded piezoelectric material is studied. The open- and closed- circuit conditions on the upper and lower face surfaces are considered. The Reissner mixed variational method is employed for solution of the corresponding 3D

*Corresponding author, Professor
E-mail: akbarov@yildiz.edu.tr
[a] Ph.D.
E-mail: fazile.cafarova@mail.ru
[b] Professor
E-mail: nazmiye@yildiz.edu.tr

ISSN: 1738-1584 (Print), 1738-1991 (Online)

problems. The refined plate theories with various order are used for reducing the 3D problems to the corresponding 2D problems and the finite layer method is employed for obtaining numerical results. The accuracy of these results is established through comparison with the corresponding ones obtained within the scope of the 3D formulation.

In the paper by Arefi and Allam (2015), the von-Karman type non-linear plate theory is employed for investigation of the response of the bi-layered circular plate made of functionally-graded piezoelectric material and resting on a Winkler-Pasternak foundation. For illustration of the geometrical non-linearity and other problem parameters on the static response of the considered system, the corresponding numerical results are presented and discussed.

The paper by Jabbary *et al*. (2013) studies the buckling of the sandwich circular plate with piezoelectric face and porous middle layers under radial compression. The Kirchhoff-Love plate theory within the scope of von-Karman geometric non-linearity is employed for this investigation. The virtual work principle is employed for obtaining the stability loss equations. The analytical expression for the critical force is obtained and according to this expression the influence of the problem parameters, as well as of the piezoelectricity of the covering layer material is determined. The results obtained in this paper are acceptable for very thin plates.

The paper by Meng *et al.* (2010) deals with the study of elliptically near-surface buckling of the piezoelectric laminated cylindrical hollow shell under electric and thermal load. The delaminated part of the shell is called the sub-shell, while the remaining part is called the base-shell. Basically, the aforementioned near surface buckling of the shell is reduced to the stability loss of the sub-shell under action of the external thermal and electrical load, the action of which is transmitted to the sub-shell through the base-shell. The investigations are made within the scope of the classical theory of shells by employing the Kirchhoff-Love hypothesis under the use of the geometrical nonlinear strain-displacement relations. Numerical results on the critical strain and on the influence of the problem parameters on this strain are presented and discussed. In particular, it is established that the effect of the applied electric field on the critical compression strain is much larger than that of the temperature changes.

It should be noted that all the foregoing investigations have been made within the scope of the approximate plate and shell theories, the accuracy of which depends significantly on the geometrical and electro-mechanical properties. Consequently, the order of the accuracy of these results can be estimated with the use of the corresponding results obtained within the scope of the 3D exact theories. For instance, the accuracy of the results related to the stability loss or buckling delamination problems can be estimated with the corresponding results obtained within the scope of the 3D exact linearized theories, the present level of which has been detailed in the monographs by Guz (1999, 2004) who made many fundamental contributions to creating this theory. This theory was also employed for investigation of the stability loss around cracks contained in homogeneous and piecewise homogeneous infinite elastic bodies. A review of the corresponding investigations is detailed in the paper by Bogdanov *et al*. (2015).

In the foregoing sense, the first attempt with respect to the buckling delamination problems related to the system comprising elastic and piezoelectric constituents was made in the paper by Akbarov and Yahnioglu (2013). More precisely, in this paper, the buckling delamination of the sandwich plate strip with piezoelectric face and elastic core layers is investigated in the plane-strain state by employing the three-dimensional linearized theory of electro-elastic stability. In this investigation it is also assumed that the plate-strip has two interface inner cracks between the face and core layers and buckling delamination of the plate takes place around these cracks.

In another paper by Akbarov and Yahnioglu (2016), the influence of the initial stresses in the aforementioned sandwich plate-strip on the total electro-mechanical potential energy and energy release rate at the interface crack tips is investigated.

The present paper deals with the study of the buckling delamination problem of the sandwich circular plate consisting of the core elastic-metal and two piezoelectric face layers. It is assumed that on the interface planes of the layers there are penny-shaped cracks and their edge surfaces have initial infinitesimal rotationally symmetric imperfections. The development of these imperfections with compression of the plate in the inward radial direction by uniformly distributed rotationally symmetric normal forces is investigated by employing the geometrical non-linear exact electro-mechanical field equations for piezoelectric and elastic materials. Numerical results on the values of the critical stresses and forces for various values of the problem parameter are presented and discussed. Note that the corresponding problems for the case where the circular plate consists of elastic and viscoelastic constituents are made in the papers by Akbarov and Rzayev (2002) and Rzayev and Akbarov (2002). The results obtained in these two papers and other related ones are also detailed in the monograph by Akbarov (2013).

2. Formulation of the problem

Consider a circular sandwich plate whose geometry is shown in Fig. 1 and for generality, assume that the materials of all the layers are piezoelectric ones. We suppose that the materials of the upper and lower face planes are the same and between the core and face layers there are penny-shaped cracks whose locations are also shown in Fig. 1.

We associate with the lower face layer of the plate the cylindrical coordinate system $Or\theta z$ (Fig. 1) and the position of the points of the plate we determine through the Lagrange coordinates in this system. Thus, according to Fig. 1, in the selected coordinate system, the plate occupies the region $\{0 \le r \le \ell / 2; 0 \le \theta \le 2\pi; 0 \le z \le h\}$ and the penny-shaped cracks occur in $\{z = h_F \pm 0;\ 0 \le r \le \ell_0 / 2\}$ and in $\{z = h_C + h_F \pm 0;\ 0 \le r \le \ell_0 / 2\}$. Besides all of these,

we assume that in the initial (natural) state the edge-surfaces of the cracks have infinitesimal rotationally symmetric imperfections. In Fig. 1(b) the upper (lower) edge of the upper and lower cracks is denoted by $S_U^+(S_U^-)$ and $S_L^+(S_L^-)$, respectively. The equations of these surfaces are given as follows

$$z = h_F \pm \varepsilon f(r) \quad \text{for} \quad S_L^{\pm} \;;\; z = h_C + h_F \pm \varepsilon f(r) \quad \text{for} \quad S_U^{\pm}, \quad \text{under} \quad 0 \le r \le \ell_0/2 \tag{1}$$

where ε (i.e, 0< ε <<1) is a parameter which characterizes the degree of the imperfections and $f(r)$ is a function which shows the mode of the imperfection.

Thus, within the framework of the foregoing assumptions, we suppose that the plate is compressed in the inward radial direction by uniformly distributed rotationally symmetric normal forces with intensity p acting on the lateral surface of the circular plate-disc. Below we will denote the values related to the upper and lower face layers by upper indices (3) and (1) respectively, whereas the values related to the core layer are denoted by (2).

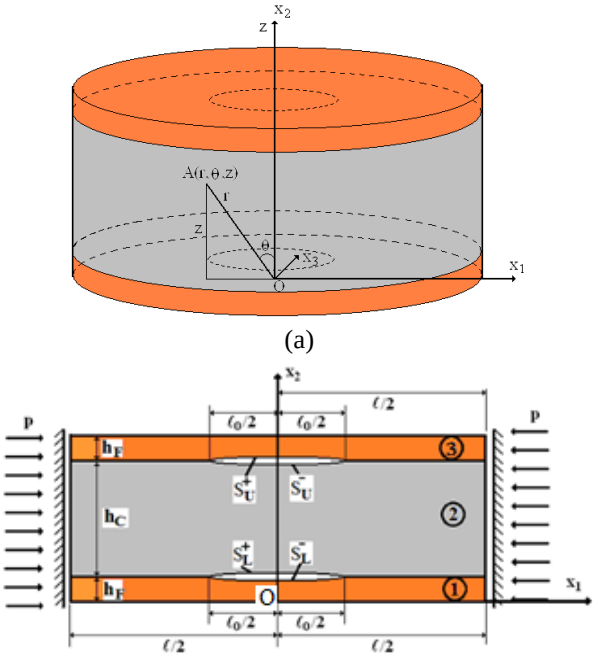

Fig. 1 The geometry of the considered circular plate with two cracks (a) and the cross section of the circular plate with loading condition and some geometric values (b): r, θ and z (x_1, x_2 and x_3) are cylindrical (Cartesian) coordinates, $\ell_0/2$ ($\ell/2$) is a Radius of the penny-shaped cracks (circular disc-plate), h_F (h_C) is a thickness of the face (core) layer, S_U^+ (S_U^-) and S_L^+ (S_L^-) upper (lower) edge surfaces of the upper and lower cracks, p is an intensity of the compressional force

As we are considering the rotationally axisymmetric deformation state, we will use the corresponding field equations related to this case. We write the exact geometrical non-linear electro-mechanical field equations which are satisfied within each plate separately.

The equilibrium equations

$$\frac{\partial t_{rr}^{(k)}}{\partial r} + \frac{\partial t_{zr}^{(k)}}{\partial z} + \frac{1}{r}(t_{rr}^{(k)} - t_{\theta\theta}^{(k)}) = 0 \;,$$

$$\frac{\partial t_{rz}^{(k)}}{\partial r} + \frac{\partial t_{zz}^{(k)}}{\partial z} + \frac{1}{r} t_{rz}^{(k)} = 0 \,, \quad \frac{\partial D_R^{(k)}}{\partial r} + \frac{1}{r} D_R^{(k)} + \frac{\partial D_Z^{(k)}}{\partial z} = 0$$

$$t_{rr}^{(k)} = \sigma_{rr}^{(k)}\left(1 + \frac{\partial u_r^{(k)}}{\partial r}\right) + \sigma_{rz}^{(k)} \frac{\partial u_r^{(k)}}{\partial z} + M_{rr}^{(k)} \,,$$

$$t_{\vartheta\theta}^{(k)} = \sigma_{\theta\theta}^{(k)}\left(1 + \frac{u_r^{(k)}}{r}\right) + M_{\theta\theta}^{(k)} \,,$$

$$t_{zr}^{(k)} = \sigma_{zr}^{(k)}\left(1 + \frac{\partial u_r^{(k)}}{\partial r}\right) + \sigma_{zz}^{(k)} \frac{\partial u_r^{(k)}}{\partial z} + M_{zr}^{(k)} \,, \tag{2}$$

$$t_{rz}^{(k)} = \sigma_{rr}^{(k)} \frac{\partial u_z^{(k)}}{\partial r} + \sigma_{rz}^{(k)}\left(1 + \frac{\partial u_z^{(k)}}{\partial z}\right) + M_{rz}^{(k)} \,,$$

$$t_{zz}^{(k)} = \sigma_{zz}^{(k)}\left(1 + \frac{\partial u_z^{(k)}}{\partial z}\right) + \sigma_{rz}^{(k)} \frac{\partial u_z^{(k)}}{\partial z} + M_{zz}^{(k)} \,,$$

$$D_R^{(k)} = \left(1 + \frac{\partial u_r^{(k)}}{\partial r}\right) D_r^{(k)} + \frac{\partial u_r^{(k)}}{\partial z} D_z^{(k)} \;,$$

$$D_Z^{(k)} = \frac{\partial u_z^{(k)}}{\partial r} D_r^{(k)} + \left(1 + \frac{\partial u_z^{(k)}}{\partial z}\right) D_z^{(k)}$$

The electro-mechanical relations for piezoelectric materials

$$\sigma_{rr}^{(k)} = c_{1111}^{(k)} s_{rr}^{(k)} + c_{1122}^{(k)} s_{\theta\theta}^{(k)} + c_{1133}^{(k)} s_{zz}^{(k)} - e_{111}^{(k)} E_r^{(k)} - e_{311}^{(k)} E_z^{(k)} \,,$$

$$\sigma_{\theta\theta}^{(k)} = c_{2211}^{(k)} s_{rr}^{(k)} + c_{2222}^{(k)} s_{\theta\theta}^{(k)} + c_{2233}^{(k)} s_{zz}^{(k)} - e_{122}^{(k)} E_r^{(k)} - e_{322}^{(k)} E_z^{(k)} \,,$$

$$\sigma_{zz}^{(k)} = c_{3311}^{(k)} s_{rr}^{(k)} + c_{3322}^{(k)} s_{\theta\theta}^{(k)} + c_{3333}^{(k)} s_{zz}^{(k)} - e_{133}^{(k)} E_r^{(k)} - e_{333}^{(k)} E_z^{(k)} \,,$$

$$\sigma_{rz}^{(k)} = c_{1311}^{(k)} s_{rz}^{(k)} - e_{113}^{(k)} E_r^{(k)} - e_{313}^{(k)} E_z^{(k)} \,,$$

$$D_r^{(k)} = e_{111}^{(k)} s_{rr}^{(k)} + e_{122}^{(k)} s_{\theta\theta}^{(k)} + e_{133}^{(k)} s_{zz}^{(k)} + \varepsilon_{11}^{(k)} E_r^{(k)} + \varepsilon_{13}^{(k)} E_z^{(k)} \,,$$

$$D_z^{(k)} = e_{311}^{(k)} s_{rr}^{(k)} + e_{322}^{(k)} s_{\theta\theta}^{(k)} + e_{333}^{(k)} s_{zz}^{(k)} + \varepsilon_{31}^{(k)} E_r^{(k)} + \varepsilon_{33}^{(k)} E_z^{(k)} \,,$$

$$M_{rr}^{(k)} = \varepsilon_0^{(k)}\left(E_r^{(k)} E_r^{(k)} - \frac{1}{2} E^{(k)}\right), \tag{3}$$

$$M_{\theta\theta}^{(k)} = \varepsilon_0^{(k)}\left(E_\theta^{(k)} E_\theta^{(k)} - \frac{1}{2} E^{(k)}\right),$$

$$M_{zz}^{(k)} = \varepsilon_0^{(k)}\left(E_z^{(k)} E_z^{(k)} - \frac{1}{2} E^{(k)}\right),$$

$$M_{rz}^{(k)} = M_{zr}^{(k)} = \varepsilon_0^{(k)}\left(E_r^{(k)} E_z^{(k)}\right)$$

$$E^{(k)} = (E_r^{(k)})^2 + (E_\theta^{(k)})^2 + (E_z^{(k)})^2 \;,\; E_r^{(k)} = -\frac{\partial \phi^{(k)}}{\partial r} \;,$$

$$E_z^{(k)} = -\frac{\partial \phi^{(k)}}{\partial z}$$

The strain-displacements relations

$$s_{rr}^{(k)}=\frac{\partial u_r^{(k)}}{\partial r}+\frac{1}{2}\left(\frac{\partial u_r^{(k)}}{\partial r}\right)^2+\frac{1}{2}\left(\frac{\partial u_z^{(k)}}{\partial r}\right)^2,$$

$$s_{\theta\theta}^{(k)}=\frac{u_r^{(k)}}{r}+\frac{1}{2}\left(\frac{u_r^{(k)}}{r}\right)^2,$$

$$s_{zz}^{(k)}=\frac{\partial u_z^{(k)}}{\partial z}+\frac{1}{2}\left(\frac{\partial u_z^{(k)}}{\partial z}\right)^2+\frac{1}{2}\left(\frac{\partial u_r^{(k)}}{\partial z}\right)^2, \tag{4}$$

$$s_{rz}^{(k)}=\frac{1}{2}\left(\frac{\partial u_r^{(k)}}{\partial z}+\frac{\partial u_z^{(k)}}{\partial r}+\frac{\partial u_r^{(k)}}{\partial z}\frac{\partial u_r^{(k)}}{\partial r}+\frac{\partial u_z^{(k)}}{\partial z}\frac{\partial u_z^{(k)}}{\partial r}\right)$$

In (2)-(4) the following notation is used: $\sigma_{rr}^{(k)}$,…, $\sigma_{rz}^{(k)}$ and $s_{rr}^{(k)}$,…, $s_{rz}^{(k)}$ are the components of the stress and Green strain tensors, respectively, $M_{rr}^{(k)}$,…, $M_{rz}^{(k)}$ are the components of the Maxwell stress tensor, $\varepsilon_0^{(k)}$ is the permittivity of free space, $u_r^{(k)}$ and $u_z^{(k)}$ are components of the displacement vector, $D_r^{(k)}$ and $D_z^{(k)}$ are the components of the electrical displacement vector, and $c_{ijkl}^{(k)}$, $e_{nij}^{(k)}$ and $\varepsilon_{nj}^{(k)}$ are the elastic, piezoelectric and dielectric constants, respectively.

Note that the piezoelectric material exhibits the characteristics of orthotropic materials with the corresponding elastic symmetry axes and becomes electrically polarized under mechanical loads or mechanical deformation placed in an electrical field. According to Yang (2005), the polled direction of the piezoelectric material will change according to the position of the material constants in the constitutive relations. In the present paper, under numerical calculations, it is assumed that the Oz axis direction is the polarized direction. Moreover, we introduce the following notation.

$$\begin{gathered}c_{1111}^{(k)}=c_{11}^{(k)},\ c_{2211}^{(k)}=c_{1122}^{(k)}=c_{12}^{(k)},\\ c_{3311}^{(k)}=c_{1133}^{(k)}=c_{13}^{(k)},\ c_{2222}^{(k)}=c_{22}^{(k)},\\ c_{3322}^{(k)}=c_{2233}^{(k)}=c_{23}^{(k)},\\ c_{3333}^{(k)}=c_{33}^{(k)},\ c_{1313}^{(k)}=c_{55}^{(k)}\quad e_{111}^{(k)}=e_{11}^{(k)},\\ e_{311}^{(k)}=e_{31}^{(k)},\ e_{122}^{(k)}=e_{12}^{(k)},\ e_{322}^{(k)}=e_{32}^{(k)},\\ e_{133}^{(k)}=e_{13}^{(k)},\ e_{333}^{(k)}=e_{33}^{(k)},\quad e_{313}^{(k)}=e_{35}^{(k)}e_{113}^{(k)}=e_{15}^{(k)}\end{gathered} \tag{5}$$

Thus, the complete geometrically non-linear electro-mechanical field equations for piezoelectric materials are the Eqs. (2)- (5).

It should be noted that in the classical linear theories of electro-elasticity the following two particularities: (I) the difference between the areas of the surface elements and the difference between the elementary volume taken before and after deformation, and (II) the rotation of the "materialized" base vectors as a result of the deformations, are not taken into consideration either under determination of the stresses and under obtaining the field equations, or under formulation of the boundary conditions with respect to the forces and the electrical displacements. However, in the case under consideration, i.e., in writing the Eqs. (2)-(4), we assume that the deformations are so small that the I peculiarity can be neglected, but the II peculiarity must be taken into consideration under determination of the stresses, electrical displacements and obtaining the field equations, and under formulation of the boundary conditions with respect to the forces and electrical displacements.

Now we formulate the boundary and contact conditions. Regarding the cracks' edges the following can be written

$$\begin{gathered}t_{rr}^{(3)}\Big|_{S_u^+}n_r^+ + t_{zr}^{(3)}\Big|_{S_u^+}n_z^+ = 0,\\ t_{rz}^{(3)}\Big|_{S_u^+}n_r^+ + t_{zz}^{(3)}\Big|_{S_u^+}n_z^+ = 0,\\ t_{rr}^{(2)}\Big|_{S_u^-}n_r^- + t_{zr}^{(2)}\Big|_{S_u^-}n_z^- = 0\ ,\\ t_{rz}^{(2)}\Big|_{S_u^-}n_r^- + t_{zz}^{(2)}\Big|_{S_u^-}n_z^- = 0,\\ t_{rr}^{(2)}\Big|_{S_L^+}n_r^+ + t_{zr}^{(2)}\Big|_{S_L^+}n_z^+ = 0,\\ t_{rz}^{(2)}\Big|_{S_L^+}n_r^+ + t_{zz}^{(2)}\Big|_{S_L^+}n_z^+ = 0,\\ t_{rr}^{(1)}\Big|_{S_L^-}n_r^- + t_{zr}^{(1)}\Big|_{S_L^-}n_z^- = 0,\\ t_{rz}^{(1)}\Big|_{S_L^-}n_r^- + t_{zz}^{(1)}\Big|_{S_L^-}n_z^- = 0\end{gathered} \tag{6}$$

Note the conditions (6) are satisfied for the region $\left[0\le r\le \ell_0/2\right]$, but for the region $\left[\ell_0/2\le r\le \ell/2\right]$ the following complete contact conditions take place between the layers of the plate

$$\begin{gathered}t_{zz}^{(3)}\Big|_{z=h_F+h_C}=t_{zz}^{(2)}\Big|_{z=h_F+h_C}\ ,\\ t_{zr}^{(3)}\Big|_{z=h_F+h_C}=t_{zr}^{(2)}\Big|_{z=h_F+h_C},\\ u_z^{(3)}\Big|_{z=h_F+h_C}=u_z^{(2)}\Big|_{z=h_F+h_C},\\ u_r^{(3)}\Big|_{z=h_F+h_C}=u_r^{(2)}\Big|_{z=h_F+h_C},\\ t_{zz}^{(2)}\Big|_{z=h_F}=t_{zz}^{(1)}\Big|_{z=h_F},\ t_{zr}^{(2)}\Big|_{z=h_F}=t_{zr}^{(1)}\Big|_{z=h_F},\\ u_z^{(2)}\Big|_{z=h_F}=u_z^{(1)}\Big|_{z=h_F},\quad u_r^{(2)}\Big|_{z=h_F}=u_r^{(1)}\Big|_{z=h_F}\end{gathered} \tag{7}$$

Moreover, on the upper surface of the upper face layer and on the lower surface of the lower face layer of the plate

the following conditions are satisfied

$$t_{zz}^{(3)}\Big|_{z=2h_F+h_C}=0,\ t_{zr}^{(3)}\Big|_{z=2h_F+h_C}=0,\ t_{zz}^{(1)}\Big|_{z=0}=0,\quad t_{zr}^{(1)}\Big|_{z=0}=0 \text{ for } 0\le r\le \ell/2 \tag{8}$$

We assume that on the lateral surface of the plate the following conditions are satisfied

$$t_{rr}^{(k)}\Big|_{r=\ell/2}=-p,\ u_z^{(k)}\Big|_{r=\ell/2}=0, \text{ for } k=1,2,3 \text{ under } 0\le z\le 2h_F+h_C \tag{9}$$

Note that (6) – (9) are written for the mechanical forces and displacements. For the electrical displacement and electrical potential we formulate the following conditions:

on the cracks' edges

$$D_Z^{(3)}\Big|_{S_u^+}=0,\ D_Z^{(2)}\Big|_{S_u^-}=0,\ D_Z^{(2)}\Big|_{S_L^+}=0,\quad D_Z^{(1)}\Big|_{S_L^-}=0, \text{ for } 0\le r\le \ell_0/2 \tag{10}$$

or

$$\phi^{(3)}\Big|_{S_u^+}=0,\ \phi^{(2)}\Big|_{S_u^-}=0,\ \phi^{(2)}\Big|_{S_L^+}=0,\ \phi^{(1)}\Big|_{S_L^-}=0 \text{ , for } 0\le r\le \ell_0/2 \tag{11}$$

on the contact regions between the layers

$$D_Z^{(3)}\Big|_{z=h_F+h_C}=D_Z^{(2)}\Big|_{z=h_F+h_C},\quad \phi^{(3)}\Big|_{z=h_F+h_C}=\phi^{(2)}\Big|_{z=h_F+h_C},$$
$$D_Z^{(2)}\Big|_{z=h_F}=D_Z^{(1)}\Big|_{z=h_F},\ \phi^{(2)}\Big|_{z=h_F}=\phi^{(2)}\Big|_{z=h_F}, \text{ for } \ell_0/2\le r\le \ell/2 \tag{12}$$

on the upper face of the upper face layer and on the lower face of the lower face layer

$$D_Z^{(3)}\Big|_{z=2h_F+h_C}=0,\ D_Z^{(1)}\Big|_{z=0}=0 \text{ for } 0\le r\le \ell/2 \tag{13}$$

or

$$\phi^{(3)}\Big|_{z=2h_F+h_C}=0,\ \phi^{(1)}\Big|_{z=0}=0 \text{ for } 0\le r\le \ell/2 \tag{14}$$

on the lateral surface of the plate

$$D_R^{(k)}\Big|_{r=\ell/2}=0, \text{ for } k=1,2,3 \text{ under } 0\le z\le 2h_F+h_C \tag{15}$$

or

$$\phi^{(k)}\Big|_{r=\ell/2}=0, \text{ for } k=1,2,3 \text{ under } 0\le z\le 2h_F+h_C \tag{16}$$

The conditions (10), (13) and (15) are called "open–circuit", however the conditions (11), (14) and (16) are called "short–circuit".

This completes the mathematical formulation of the problem, according to which it is required to investigate the development of the initial imperfections of the penny-shaped cracks' edges with the compressional uniformly distributed rotationally symmetric normal forces acting on the lateral surface of the plate.

3. Method of solution

3.1 Presentation of the sought values in series form with respect to the small parameter

For the solution of the problem formulated in the previous section we employ the approach developed in the monograph by Akbarov (2013) for purely elastic and viscoelastic materials, according to which, all the sought values are presented in the series form in the small parameter ε which enters into the expressions in (1):

$$\left\{\sigma_{rr}^{(k)},...,u_r^{(k)},...,D_r^{(k)},...,\phi^{(k)}\right\}=\sum_{n=0}^{\infty}\varepsilon^n\left\{\sigma_{rr}^{(k),n},...,u_r^{(k),n},...,D_r^{(k),n},...,\phi^{(k),n}\right\} \tag{17}$$

Obtaining the expressions for the components $n_r^{\pm}$ and $n_z^{\pm}$ of the normal vector to the cracks' edge surfaces in (1) and representing these expressions also in the series form in the small parameter ε, and substituting these and the expressions in (17) into the foregoing non-linear equations and relations, and doing some cumbersome mathematical manipulations, we obtain the corresponding equations and relations for determination of each approximation in (17). Here we write these equations and relations only for the zeroth and first approximations and under consideration of the zeroth approximation we neglect the non-linear terms.

Thus, the equations and relations for the zeroth approximations are

$$\frac{\partial\sigma_{rr}^{(k),0}}{\partial r}+\frac{\partial\sigma_{zr}^{(k),0}}{\partial z}+\frac{1}{r}(\sigma_{rr}^{(k),0}-\sigma_{\theta\theta}^{(k),0})=0,\quad \frac{\partial\sigma_{rz}^{(k),0}}{\partial r}+\frac{\partial\sigma_{zz}^{(k),0}}{\partial z}+\frac{1}{r}\sigma_{rz}^{(k),0}=0,\quad \frac{\partial D_r^{(k),0}}{\partial r}+\frac{1}{r}D_r^{(k),0}+\frac{\partial D_z^{(k),0}}{\partial z}=0 \tag{18}$$

$$s_{rr}^{(k),0}=\frac{\partial u_r^{(k),0}}{\partial r},\ s_{\theta\theta}^{(k),0}=\frac{u_r^{(k),0}}{r},\quad s_{zz}^{(k),0}=\frac{\partial u_z^{(k),0}}{\partial z},\ s_{rz}^{(k),0}=\frac{1}{2}\left(\frac{\partial u_r^{(k),0}}{\partial z}+\frac{\partial u_z^{(k),0}}{\partial r}\right), \tag{19}$$

$$\sigma_{zr}^{(3),0}\Big|_{z=h_F+h_C}=0\,,\ \ \sigma_{zz}^{(3),0}\Big|_{z=h_F+h_C}=0\,,$$
$$\sigma_{zr}^{(2),0}\Big|_{z=h_F+h_C}=0\ \ ,\ \ \sigma_{zz}^{(2),0}\Big|_{z=h_F+h_C}=0$$

$$\sigma_{zr}^{(2),0}\Big|_{z=h_F}=0\qquad \sigma_{zz}^{(2),0}\Big|_{z=h_F}=0\,,$$
$$\sigma_{zr}^{(1),0}\Big|_{z=h_F}=0\,,\ \ \sigma_{zz}^{(1),0}\Big|_{z=h_F}=0\,,\ \text{for}\ \ 0\le r\le \ell_0/2 \tag{20}$$

$$\sigma_{zz}^{(3),0}\Big|_{z=h_F+h_C}=\sigma_{zz}^{(2),0}\Big|_{z=h_F+h_C}\ \ ,$$
$$\sigma_{zr}^{(3),0}\Big|_{z=h_F+h_C}=\sigma_{zr}^{(2),0}\Big|_{z=h_F+h_C}\,,$$
$$u_z^{(3),0}\Big|_{z=h_F+h_C}=u_z^{(2),0}\Big|_{z=h_F+h_C}\,,$$
$$u_r^{(3),0}\Big|_{z=h_F+h_C}=u_r^{(2),0}\Big|_{z=h_F+h_C}\,, \tag{21}$$
$$\sigma_{zz}^{(2),0}\Big|_{z=h_F}=\sigma_{zz}^{(1),0}\Big|_{z=h_F}\,,\ \ \sigma_{zr}^{(2),0}\Big|_{z=h_F}=\sigma_{zr}^{(1),0}\Big|_{z=h_F}\,,$$
$$u_z^{(2),0}\Big|_{z=h_F}=u_z^{(1),0}\Big|_{z=h_F}\,,$$
$$u_r^{(2),0}\Big|_{z=h_F}=u_r^{(1),0}\Big|_{z=h_F}\,,\qquad \text{for}\ \ \ell_0/2\le r\le \ell/2$$

$$\sigma_{zz}^{(3),0}\Big|_{z=2h_F+h_C}=0\,,\ \ \sigma_{zr}^{(3),0}\Big|_{z=2h_F+h_C}=0\,,$$
$$\sigma_{zz}^{(1),0}\Big|_{z=0}=0\,,\ \ \sigma_{zr}^{(1),0}\Big|_{z=0}=0\ \ \text{for}\ \ 0\le r\le \ell/2 \tag{22}$$

$$\sigma_{rr}^{(k),0}\Big|_{r=\ell/2}=-p\,,\ \ u_z^{(k),0}\Big|_{r=\ell/2}=0\,,\ \text{for}\ \ k=1,2,3 \tag{23}$$
$$\text{under}\ \ 0\le z\le 2h_F+h_C$$

$$D_z^{(3),0}\Big|_{z=h_F+h_C}=0\,,\ \ D_z^{(2),0}\Big|_{z=h_F+h_C}=0\,,$$
$$D_z^{(2),0}\Big|_{z=h_F}=0\,, \tag{24}$$
$$D_z^{(1),0}\Big|_{z=h_F}=0\,,\ \text{for}\ \ 0\le r\le \ell_0/2$$

or

$$\phi^{(3),0}\Big|_{z=h_F+h_C}=0\,,\ \ \phi^{(2),0}\Big|_{z=h_F+h_C}=0\,, \tag{25}$$
$$\phi^{(2),0}\Big|_{z=h_F}=0\,,\ \ \phi^{(1),0}\Big|_{z=h_F}=0\,,\ \text{for}\ \ 0\le r\le \ell_0/2$$

$$D_z^{(3),0}\Big|_{z=h_F+h_C}=D_z^{(2),0}\Big|_{z=h_F+h_C}\,,$$
$$\phi^{(3),0}\Big|_{z=h_F+h_C}=\phi^{(2),0}\Big|_{z=h_F+h_C}\,,$$
$$D_z^{(2),0}\Big|_{z=h_F}=D_z^{(1),0}\Big|_{z=h_F}\,, \tag{26}$$
$$\phi^{(2),0}\Big|_{z=h_F}=\phi^{(2),0}\Big|_{z=h_F}\,,\qquad \text{for}\ \ \ell_0/2\le r\le \ell/2$$

$$D_z^{(3),0}\Big|_{z=2h_F+h_C}=0\,,\ \ D_z^{(1),0}\Big|_{z=0}=0\ \ \text{for}\ \ 0\le r\le \ell/2 \tag{27}$$

or

$$\phi^{(3),0}\Big|_{z=2h_F+h_C}=0\,,\ \ \phi^{(1),0}\Big|_{z=0}=0\ \ \text{for}\ \ 0\le r\le \ell/2 \tag{28}$$

$$D_r^{(k),0}\Big|_{r=\ell/2}=0\,,\quad \text{for}\ \ k=1,2,3\ \ \text{under} \tag{29}$$
$$0\le z\le 2h_F+h_C$$

or

$$\phi^{(k),0}\Big|_{r=\ell/2}=0\,,\quad \text{for}\ \ k=1,2,3\ \ \text{under} \tag{30}$$
$$0\le z\le 2h_F+h_C$$

Note that the equations and relations (18)-(30) are obtained from the Eqs. (2), (4), (6)-(16), respectively.

Now we consider the equations and relations obtained for the first approximation. Under obtaining these equations and relations we assume that $\sigma_{rz}^{(k),0}=\sigma_{zz}^{(k),0}=0$ and $\left\{\partial u_r^{(k),0}/\partial r\ \ ;\ \ \partial u_z^{(k),0}/\partial r\ \ ;\ \ \partial u_r^{(k),0}/\partial z\ \ ;\right.$ $\left.\partial u^{(k),0}/\partial z\right\}<<1$ and we neglect these terms with respect to 1. Thus, for the first approximation we obtain the following equations and relations.

$$\frac{\partial t_{rr}^{(k),1}}{\partial r}+\frac{\partial t_{zr}^{(k),1}}{\partial z}+\frac{1}{r}(t_{rr}^{(k),1}-t_{\theta\theta}^{(k),1})=0\ \ ,$$
$$\frac{\partial t_{rz}^{(k),1}}{\partial r}+\frac{\partial t_{zz}^{(k),1}}{\partial z}+\frac{1}{r}t_{rz}^{(k),1}=0\,,$$
$$\frac{\partial D_R^{(k),1}}{\partial r}+\frac{1}{r}D_R^{(k),1}+\frac{\partial D_Z^{(k),1}}{\partial z}=0\,, \tag{31}$$
$$t_{rr}^{(k)}=\sigma_{rr}^{(k),1}+\sigma_{rr}^{(k),0}\frac{\partial u_r^{(k),1}}{\partial r}+M_{rr}^{(k),1}\,,$$
$$t_{\vartheta\theta}^{(k),1}=\sigma_{\theta\theta}^{(k),1}+\sigma_{\theta\theta}^{(k),0}\frac{u_r^{(k),1}}{r}+M_{\theta\theta}^{(k),1}\,,$$

$$t_{zr}^{(k)} = \sigma_{zr}^{(k),1} + M_{zr}^{(k),1},$$
$$t_{rz}^{(k),1} = \sigma_{rz}^{(k),1} + \sigma_{rr}^{(k),0}\frac{\partial u_z^{(k),1}}{\partial r} + M_{rz}^{(k),1},$$

$$t_{zz}^{(k),1} = \sigma_{zz}^{(k),1} + M_{zz}^{(k),1},$$
$$D_R^{(k),1} = D_r^{(k),1} + D_r^{(k),0}\frac{\partial u_r^{(k),1}}{\partial r} + \frac{\partial u_r^{(k),1}}{\partial z}D_z^{(k),0},$$

$$D_Z^{(k),1} = D_z^{(k),1} + D_z^{(k),0}\frac{\partial u_z^{(k),1}}{\partial z} + D_r^{(k),0}\frac{\partial u_z^{(k),1}}{\partial r},$$

$$M_{rr}^{(k),1} = E_r^{(k),0}E_r^{(k),1} - E_\theta^{(k),0}E_\theta^{(k),1} - E_z^{(k),0}E_z^{(k),1},$$

$$M_{\theta\theta}^{(k),1} = E_\theta^{(k),0}E_\theta^{(k),1} - E_r^{(k),0}E_r^{(k),1} - E_z^{(k),0}E_z^{(k),1},$$

$$M_{zz}^{(k),1} = E_z^{(k),0}E_z^{(k),1} - E_\theta^{(k),0}E_\theta^{(k),1} - E_r^{(k),0}E_r^{(k),1}$$

$$s_{rr}^{(k),1} = \frac{\partial u_r^{(k),1}}{\partial r}, \quad s_{\theta\theta}^{(k),1} = \frac{u_r^{(k),1}}{r}, \quad s_{zz}^{(k),1} = \frac{\partial u_z^{(k),1}}{\partial z},$$
$$s_{rz}^{(k),1} = \frac{1}{2}\left(\frac{\partial u_r^{(k),1}}{\partial z} + \frac{\partial u_z^{(k),1}}{\partial r}\right),$$

$$t_{zr}^{(3),1}\Big|_{z=h_F+h_C} = \frac{df(r)}{dr}\sigma_{rr}^{(3),0}\Big|_{z=h_F+h_C}, \qquad (32)$$
$$t_{rr}^{(3),1}\Big|_{z=h_F+h_C} = 0,$$
$$t_{zr}^{(2),1}\Big|_{z=h_F+h_C} = \frac{df(r)}{dr}\sigma_{rr}^{(2),0}\Big|_{z=h_F+h_C},$$

$$t_{rr}^{(2),1}\Big|_{z=h_F+h_C} = 0, \quad t_{zr}^{(2),1}\Big|_{z=h_F} = \frac{df(r)}{dr}\sigma_{rr}^{(2),0}\Big|_{z=h_F},$$
$$t_{rr}^{(2),1}\Big|_{z=h_F} = 0,$$
$$t_{zr}^{(1),1}\Big|_{z=h_F} = \frac{df(r)}{dr}\sigma_{rr}^{(1),0}\Big|_{z=h_F}, \quad t_{rr}^{(1),1}\Big|_{z=h_F} = 0, \qquad (33)$$
$$\text{for } 0 \le r \le \ell_0/2$$

$$t_{zz}^{(3),1}\Big|_{z=h_F+h_C} = t_{zz}^{(2),1}\Big|_{z=h_F+h_C},$$
$$t_{zr}^{(3),1}\Big|_{z=h_F+h_C} = t_{zr}^{(2),1}\Big|_{z=h_F+h_C},$$
$$u_z^{(3),1}\Big|_{z=h_F+h_C} = u_z^{(2),1}\Big|_{z=h_F+h_C}, \qquad (34)$$
$$u_r^{(3),1}\Big|_{z=h_F+h_C} = u_r^{(2),1}\Big|_{z=h_F+h_C},$$
$$t_{zz}^{(2),1}\Big|_{z=h_F} = t_{zz}^{(1),1}\Big|_{z=h_F}, \quad t_{zr}^{(2),1}\Big|_{z=h_F} = t_{zr}^{(1),1}\Big|_{z=h_F},$$
$$u_z^{(2),1}\Big|_{z=h_F} = u_z^{(1),1}\Big|_{z=h_F}, \quad u_r^{(2),1}\Big|_{z=h_F} = u_r^{(1),1}\Big|_{z=h_F},$$
$$\text{for } \ell_0/2 \le r \le \ell/2$$

$$t_{zz}^{(3),1}\Big|_{z=2h_F+h_C} = 0, \quad t_{zr}^{(3),1}\Big|_{z=2h_F+h_C} = 0,$$
$$t_{zz}^{(1),1}\Big|_{z=0} = 0, \quad t_{zr}^{(1),1}\Big|_{z=0} = 0 \quad \text{for } 0 \le r \le \ell/2 \qquad (35)$$

$$t_{rr}^{(k),1}\Big|_{r=\ell/2} = 0, \quad u_z^{(k),1}\Big|_{r=\ell/2} = 0, \text{ for } k = 1,2,3 \qquad (36)$$
$$\text{under } 0 \le z \le 2h_F + h_C$$

$$D_Z^{(3),1}\Big|_{z=h_F+h_C} = -\frac{\partial D_Z^{(3),0}}{\partial z}\Big|_{z=h_F+h_C} f(r),$$
$$D_Z^{(2),1}\Big|_{z=h_F+h_C} = -\frac{\partial D_Z^{(2),0}}{\partial z}\Big|_{z=h_F+h_C} f(r),$$
$$D_Z^{(2),1}\Big|_{z=h_F} = -\frac{\partial D_Z^{(2),0}}{\partial z}\Big|_{z=h_F} f(r), \qquad (37)$$
$$D_Z^{(1),1}\Big|_{z=h_C} = -\frac{\partial D_Z^{(1),0}}{\partial z}\Big|_{z=h_F} f(r), \quad \text{for } 0 \le r \le \ell_0/2$$

or

$$\phi^{(3),1}\Big|_{z=h_F+h_C} = -\frac{\partial \phi^{(3),0}}{\partial z}\Big|_{z=h_F+h_C} f(r),$$
$$\phi^{(2),1}\Big|_{z=h_F+h_C} = -\frac{\partial \phi^{(2),0}}{\partial z}\Big|_{z=h_F+h_C} f(r), \qquad (38)$$
$$\phi^{(2),1}\Big|_{z=h_F} = -\frac{\partial \phi^{(2),0}}{\partial z}\Big|_{z=h_F} f(r),$$
$$\phi^{(1),1}\Big|_{z=h_F} = -\frac{\partial \phi^{(1),0}}{\partial z}\Big|_{z=h_F} f(r), \text{ for } 0 \le r \le \ell_0/2$$

$$D_Z^{(3),1}\Big|_{z=h_F+h_C} = D_Z^{(2),1}\Big|_{z=h_F+h_C},$$
$$\phi^{(3),1}\Big|_{z=h_F+h_C} = \phi^{(2),1}\Big|_{z=h_F+h_C}, \qquad (39)$$
$$D_Z^{(2),1}\Big|_{z=h_F} = D_Z^{(1),1}\Big|_{z=h_F}, \quad \phi^{(2),1}\Big|_{z=h_F} = \phi^{(2),1}\Big|_{z=h_F}$$

$$, \quad \text{for} \quad \ell_0/2 \le r \le \ell/2$$

$$D_Z^{(3),1}\Big|_{z=2h_F+h_C} = 0\,, \quad D_Z^{(1),1}\Big|_{z=0} = 0 \quad \text{for} \quad 0 \le r \le \ell/2 \tag{40}$$

or

$$\phi^{(3),1}\Big|_{z=2h_F+h_C} = 0\,, \quad \phi^{(1)}\Big|_{z=0} = 0 \quad \text{for} \quad 0 \le r \le \ell/2 \tag{41}$$

$$D_R^{(k),1}\Big|_{r=\ell/2} = 0\,, \quad \text{for} \quad k=1,2,3 \ \text{under} \quad 0 \le z \le 2h_F + h_C \tag{42}$$

$$\phi^{(k),1}\Big|_{r=\ell/2} = 0\,, \quad \text{for} \quad k=1,2,3 \ \text{under} \quad 0 \le z \le 2h_F + h_C \tag{43}$$

Note that the equations (31)-(43) are obtained from the Eqs. (2), (4), (6)-(16), respectively. Direct verification shows that the system of Eqs. (31)-(43) coincides with the corresponding ones of the three-dimensional linearized theory of electro-elastic stability which are detailed, for instance, in the monographs by Yang (2005), Guz (1999), Akbarov (2013) etc.

It is also necessary to add to the system of equations related to the zeroth and first approximations the corresponding constitutive relations obtained from (3). As the relations in (3) are linear ones, therefore the constitutive relations of each approximation are as in (3).

This completes consideration of the equations and relations related to the zeroth and first approximations in the series expansion (17). As shown in the monograph by Akbarov (2013), as well as in related papers, such as Akbarov and Rzayev (2002) and Rzayev and Akbarov (2002), for determination of the critical parameters which determine the buckling delamination of the circular plate under consideration, the solutions obtained within the scope of the zeroth and first approximations are enough.

Now we consider determination of the quantities related to the zeroth and first approximations.

3.2 Determination of the values related to the zeroth approximation

First of all, we note that the zeroth approximation corresponds to the case where the plate under consideration with the cracks without any imperfection on their edge surfaces, is compressed with a uniformly distributed rotationally symmetric normal compressive force with intensity p acting on the lateral surface of the plate in the inward radial direction. It is known that, according to Saint Venant's principle, in the region where $0 \le r < \ell/2 - h$ the stress-strain state can be taken as homogeneous with very high accuracy. In other words, in this region we can assume that

$$\begin{gathered}\sigma_{zz}^{(k),0} = 0\,, \sigma_{rz}^{(k),0} = 0\,, s_{zz}^{(k),0} = 0\,, \\ s_{rr}^{(k),0} = s_{\theta\theta}^{(k),0} = const_k\,, \\ \sigma_{rr}^{(k),0} = \sigma_{\theta\theta}^{(k),0} = const_{1k}\end{gathered} \tag{44}$$

Consequently, in the zeroth approximation in the cases where $\ell_0/2 < \ell/2 - h$ under the considered type of external loading, the existence of the cracks does not cause any stress concentration or any influence on the stress state given by the relations in (44). Taking this statement into consideration, under determination of the quantities related to the first approximation we will use the expressions given in (44).

As in the present paper, we will analyze the numerical results related only to the open-circuit case in the planes $z = 2h_F + h_C$, $h_F + h_C$, h_F and 0, and to the short-circuit case on the lateral surface $r = \ell/2$ of the plate. Therefore, in the zeroth approximation we obtain that

$$D_z^{(k),0} = D_r^{(k),0} = 0\,, \quad k = 1,2,3 \tag{45}$$

Using the constitutive relations in (3), we obtain from (45) that

$$\begin{aligned}E_r^{(k),0} &= a_1^{(k)} s_{rr}^{(k),0} + b_1^{(k)} s_{zz}^{(k),0}\,, \\ E_z^{(k),0} &= d_1^{(k)} s_{rr}^{(k),0} + c_1^{(k)} s_{zz}^{(k),0}\end{aligned} \tag{46}$$

where

$$\begin{gathered}a_1^{(k)} = \frac{\varepsilon_{13}^{(k)}(e_{31}^{(k)} + e_{32}^{(k)}) - \varepsilon_{33}^{(k)}(e_{11}^{(k)} + e_{22}^{(k)})}{\varepsilon_{11}^{(k)}\varepsilon_{33}^{(k)} - \varepsilon_{13}^{(k)}\varepsilon_{31}^{(k)}}\,, \\ b_1^{(k)} = \frac{\varepsilon_{13}^{(k)} e_{33}^{(k)} - \varepsilon_{33}^{(k)} e_{13}^{(k)}}{\varepsilon_{11}^{(k)}\varepsilon_{33}^{(k)} - \varepsilon_{13}^{(k)}\varepsilon_{31}^{(k)}}\,, \\ d_1^{(k)} = \frac{\varepsilon_{11}^{(k)}(e_{31}^{(k)} + e_{32}^{(k)}) - \varepsilon_{31}^{(k)}(e_{11}^{(k)} + e_{12}^{(k)})}{\varepsilon_{13}^{(k)}\varepsilon_{31}^{(k)} - \varepsilon_{11}^{(k)}\varepsilon_{33}^{(k)}}\,, \\ c_1^{(k)} = \frac{\varepsilon_{11}^{(k)} e_{33}^{(k)} - \varepsilon_{31}^{(k)} e_{13}^{(k)}}{\varepsilon_{13}^{(k)}\varepsilon_{31}^{(k)} - \varepsilon_{11}^{(k)}\varepsilon_{33}^{(k)}}\end{gathered} \tag{47}$$

Taking into consideration the relation $\sigma_{zz}^{(k),0} = 0$, we obtain

$$\begin{gathered}s_{zz}^{(k),0} = a_{zr}^{(k)} s_{rr}^{(k),0}\,, \\ a_{zr}^{(k)} = \frac{c_{31}^{(k)} + c_{32}^{(k)} - e_{13}^{(k)} a_1^{(k)} - e_{33}^{(k)} d_1^{(k)}}{c_{33}^{(k)} - e_{13}^{(k)} b_1^{(k)} - e_{33}^{(k)} c_1^{(k)}}\end{gathered} \tag{48}$$

Using the relation (48) it is obtained that

$$\sigma_{rr}^{(k),0} = A_r^{(k)} s_{rr}^{(k),0} \quad , \tag{49}$$

$$A_r^{(k)} = c_{11}^{(k)} + c_{12}^{(k)} - e_{11}^{(k)} a_1^{(k)} + a_{zr}^{(k)} c_{13}^{(k)} - a_{zr}^{(k)} e_{11}^{(k)} b_1^{(k)} - a_{zr}^{(k)} e_{31}^{(k)} c_1^{(k)}$$

Assuming that

$$s_{rr}^{(1),0} = s_{rr}^{(2),0}, \quad 2h_f \sigma_{rr}^{(1),0} + h_C \sigma_{rr}^{(2),0} = hp \tag{50}$$

The following expression is obtained for the stress in the face layers

$$\sigma_{rr}^{(1),0} = p\left(2\frac{h_F}{h} + \frac{h_C}{h}\frac{A_r^{(2)}}{A_r^{(1)}} \right)^{-1} \tag{51}$$

Thus, through the expressions (44)-(51) we determine completely the quantities related to the zeroth approximation. We recall that these expressions are valid for the region where $(\ell/2-h) \le r < \ell/2$ and it is assumed that the materials of the face layers are the same.

3.3 Determination of the values related to the first approximation

For determination of the first approximation we employ the FEM method and for this purpose, according to Guz (1999), Yang (2005), Akbarov (2013) and others, we introduce the following functional.

$$\Pi(u_r^{(1),1}, u_r^{(2),1}, u_r^{(3),1}, u_z^{(1),1}, u_z^{(2),1}, u_z^{(3),1}, \phi^{(1),1}, \phi^{(2),1}, \phi^{(3),1}) =$$

$$\frac{1}{2}\sum_{k=1}^{3} \iint_{\Omega^{(k)}} \left[t_{rr}^{(k),1}\frac{\partial u_r^{(k),1}}{\partial r} + t_{\theta\theta}^{(k),1}\frac{u_r^{(k),1}}{r} + t_{rz}^{(k),1}\frac{\partial u_z^{(k),1}}{\partial r} + t_{zr}^{(k),1}\frac{\partial u_r^{(k),1}}{\partial z} + \right.$$

$$\left. t_{zz}^{(k),1}\frac{\partial u_z^{(k),1}}{\partial z} + E_r^{(k),1} D_r^{(k),1} + E_z^{(k),1} D_z^{(k),1} \right] r dr dz -$$

$$\int_0^{\ell_0/2} \frac{df}{dr}\sigma_{rr}^{(1),0}\, u_r^{(1),1}\Big|_{z=h_F} r dr - \int_0^{\ell_0/2} \frac{df}{dr}\sigma_{rr}^{(2),0}\, u_r^{(2),1}\Big|_{z=h_F} r dr -$$

$$\int_0^{\ell_0/2} \frac{df}{dr}\sigma_{rr}^{(2),0}\, u_r^{(2),1}\Big|_{z=h_F+h_C} r dr - \int_0^{\ell_0/2} \frac{df}{dr}\sigma_{rr}^{(3),0}\, u_r^{(3),1}\Big|_{z=h_F+h_C} r dr \tag{52}$$

where

$$\Omega^{(1)} = \{0 \le r \le \ell/2; 0 \le z \le h_F - (z = h_F + 0; 0 \le r \le \ell_2/2)\}$$

$$\Omega^{(1)} = \{0 \le r \le \ell/2; h_F \le z \le h_F + h_C - (z = h_F + 0; 0 \le r \le \ell_2/2) - (z = h_F + h_C - 0; 0 \le r \le \ell_2/2)\} \tag{53}$$

$$\Omega^{(3)} = \{0 \le r \le \ell/2; h_F + h_C \le z \le 2h_F + h_C - (z = h_F + h_C - 0; 0 \le r \le \ell_2/2)\}$$

From equating to zero the first variation of the functional (52), i.e., from the relation

$$\delta\Pi = \sum_{k=1}^{3}\frac{\partial\Pi}{\partial u_r^{(k),1}}\delta u_r^{(k),1} + \sum_{k=1}^{3}\frac{\partial\Pi}{\partial u_z^{(k),1}}\delta u_z^{(k),1} + \sum_{k=1}^{3}\frac{\partial\Pi}{\partial \phi^{(k),1}}\delta\phi^{(k),1} = 0 \tag{54}$$

and after well-known mathematical manipulations we obtain the first three equations in (31). The boundary and contact conditions in (33)-(42) are given with respect to the forces and electrical displacements. In this way it is proven that the first three equations in (31) are the Euler equations for the functional (53) and the boundary and contact conditions in (52)-(53) which are given with respect to the forces and electrical displacements, are the related natural boundary and contact conditions.

According to FEM modelling, the solution domains indicated in (53) are divided into a finite number of finite elements. For the considered problem each of the finite elements is selected as a standard rectangular Lagrange family quadratic finite element (i.e., with nine nodes) and each node has three degrees of freedom, i.e., radial displacement $u_r^{(k),1}$, transverse displacement $u_z^{(k),1}$ and electric potential $\phi^{(k),1}$. Employing the standard Ritz technique detailed in many references, for instance, in the book by Zienkiewicz and Taylor (1989), we determine the displacements and electrical potential at the selected nodes. After this determination, by employing the initial imperfection criterion

$$\left|u_z^{(1),1}\right|_{\substack{z=h_F+h_C \\ z=0}} = \left|u_z^{(3),1}\right|_{\substack{z=h_F \\ z=0}} \to \infty \quad \text{as} \quad p \to p_{cr} \tag{55}$$

the values of the critical compressional forces are determined.

Note that the approach developed in the present paper can also be applied for buckling delamination problems related to structures containing time-dependent constituents, for instance, visco-piezoelectric materials.

This completes the consideration of the method of solution.

4. Numerical results and discussions

4.1 The selection of the initial imperfection mode and the layers' materials

As also noted above, we assume that the initial imperfection of the cracks' edges is rotationally symmetric and according to this assumption, the imperfection can be selected as follows

$$\varepsilon f(r) = s\ell_0 \cos^2\left(\frac{\pi r}{\ell_0}\right) = L\cos^2\left(\frac{\pi r}{\ell_0}\right), \quad 0 \le r \le \ell_0/2, \quad L << \ell_0, \quad \varepsilon = \frac{L}{\ell_0} \tag{56}$$

where L is the maximum value of the lift of the initial imperfection.

As a result of the selected buckling delamination criterion (55), the values of the critical parameters cannot depend on the rotationally symmetric initial imperfection mode, and this statement was also noted in the monograph by Akbarov (2013).

Note that in the present paper, the piezoelectric materials PZT -4, PZT -5H and BaTiO3 are taken as the face layer materials, however the metal materials - aluminum (Al) and steel (St) are taken as the core layer materials. The values of the elastic, piezoelectric and dielectric constants of the selected piezoelectric materials and the references used are given in Table 1.

Table 1 The values of the mechanical, piezoelectrical and dielectrical constants of the selected piezoelectric materials: here $c_{11}^{(r_1)}$,..., $c_{66}^{(r_1)}$ are elastic constants , $e_{31}^{(r_1)}$,..., $e_{15}^{(r_1)}$ are piezoelectric constants, $\varepsilon_{11}^{(r_1)}$ and $\varepsilon_{33}^{(r_1)}$ are dielectric constants

Mater. (Source Ref.)	$c_{11}^{(r_1)}$	$c_{12}^{(r_1)}$	$c_{13}^{(r_1)}$	$c_{33}^{(r_1)}$	$c_{44}^{(r_1)}$	$c_{66}^{(r_1)}$	$e_{31}^{(r_1)}$	$e_{33}^{(r_1)}$	$e_{15}^{(r_1)}$	$\varepsilon_{11}^{(r_1)}$	$\varepsilon_{33}^{(r_1)}$
PZT-4 (Yang 2005)	13.9	7.78	7.40	11.5	2.56	3.06	-5.2	15.1	12.7	0.646	0.562
PZT-5H (Yang 2005)	12.6	7.91	8.39	11.7	2.30	2.35	-6.5	23.3	17.0	1.505	1.302
BaTiO3 (Kuna 2006)	16.6	7.66	7.75	16.2	4.29	4.29	-4.4	18.6	11.6	1.434	1.682
	$\times 10^{10}\, N/m^2$						C/m^2		$\times 10^{-8}\, C/Vm$		

Table 2 The values of $p_{cr}/(\eta^{(1)}E^{(1)}+\eta^{(2)}E^{(2)})$ obtained for various $E^{(2)}/E^{(1)}$ under $\eta^{(2)}=0.3$, $2h_F/\ell_0=1/8$, $(\ell-\ell_0)/(2\ell)=0.25$ and $h_F/(2\ell)=0.03215$: here $\eta^{(1)}$ ($\eta^{(2)}$) is a volumetric concentration of the matrix (reinforcing) layers, $E^{(1)}$ ($E^{(2)}$) is a modulus of elasticity of the matrix (reinforcing) layers

$E^{(2)}/E^{(1)}$	Guz and Nazarenko (1985)	Rzayev and Akbarov (2002)	present
1	0.0167	0.0178	0.0171
10	0.0140	0.0154	0.0148
25	0.0126	0.0129	0.0120

According to Guz (2004), the values of Lame's constants of the core layer material is selected as follows: for the Al: $\lambda=48.1GPa$ and $\mu=27.1GPa$; for the St: $\lambda=92.6GPa$ and $\mu=77.5GPa$.

4.2 Testing of the FEM modelling and PC programs

Under FEM modelling using the symmetry with respect to the plane $z=h_F+h_C/2$ and the axial symmetry with respect to the Oz (Fig. 1(a)) axis of the mechanical and geometrical properties of the plate, we consider only the region $\{0\le r\le \ell/2;\ 0\le z\le h_F+h_C/2\}$ and this region is divided into 40 finite elements along the radial direction and 12 finite elements along the plate's thickness direction, resulting in 6038 NDOF Such selection of the finite elements numbers is established according to the convergence of the numerical results. All the corresponding PC programs are composed by the authors of the paper.

Now we consider testing of the aforementioned algorithm and PC programs and as in the papers by Guz and Nazarenko (1985) and Akbarov and Rzayev (2002), we consider the case where the plate material is homogeneous transverse-isotropic with the Oz symmetry axis and with effective mechanical constants where the plate material is multilayered consisting of two alternating isotropic layers with modulus of elasticity $E^{(1)}$ and $E^{(2)}$, Poisson ratio $\nu^{(1)}$ and $\nu^{(2)}$, and volumetric concentration $\eta^{(1)}$ and $\eta^{(2)}$. We note that in the paper by Guz and Nazarenko (1985), the case is considered where the semi-infinite half-space with a near-surface penny-shaped crack is compressed in the radial inward direction at infinity and the corresponding eigenvalue problem is solved by employing the dual integral equations method. According to physico-mechanical considerations, in the cases where $\ell_0 << \ell$ the results obtained for the corresponding finite region must be very near to the corresponding ones obtained in the paper by Guz and Nazarenko (1985). This fact was also checked in the paper by Akbarov and Rzayev (2002). Thus, we compare the results related to $p_{cr}/(\eta^{(1)}E^{(1)}+\eta^{(2)}E^{(2)})$ obtained for various $E^{(2)}/E^{(1)}$ in the foregoing papers and in the present paper in the case where $\eta^{(2)}=0.3$, $2h_F/\ell_0=1/8$ and $(\ell-\ell_0)/(2\ell)=0.25$. The comparison of the corresponding results given in Table 2 shows that the numerical results obtained by employing the present PC programs are very near to those obtained in the papers by Guz and Nazarenko (1985) and Akbarov and Rzayev (2002).

We also consider comparison of the results obtained by employing the present PC and FEM modeling with the corresponding ones obtained in the paper by Rzayev and Akbarov (2002) in which the buckling delamination of the circular sandwich plate with penny-shaped interface cracks was considered. However, in the paper by Rzayev and Akbarov (2002) the materials of the layers of the plate are taken as elastic ones and it is assumed that on the lateral surface of the plate, not only the displacement $u_z^{(k),1}$ but also the displacement $u_r^{(k),1}$ is equated to zero. Consequently, according to this statement the system considered in the paper by Rzayev and Akbarov (2002) must be more rigid than the corresponding one considered in the present paper and as a result of this difference, the critical values of the compressive forces obtained in the paper by Rzayev and Akbarov (2002) must be greater than the corresponding ones obtained in the present paper. These predictions are proven with the data given in Table 3 which shows the values of $p_{cr}/E^{(1)}$ obtained for various values

of $(\ell-\ell_0)/(2\ell)$ and h_F/ℓ under $2h_F/\ell_0=1/8$ and $E^{(2)}/E^{(1)}=50$. It should also be noted that the number of finite elements used in the present approach is two times greater than that used in the paper by Rzayev and Akbarov (2002) and this fact may also reduce the values of $p_{cr}/E^{(1)}$ obtained by employing the present approach. At the same time, the results given in Table 3 can also be taken as validation of the numerical results with the finite element numbers.

Thus, with this we restrict ourselves to consideration of the validation of the PC programs and FEM modelling used. Unfortunately we have not found any results of other authors related to the subject of the present paper in order to compare corresponding numerical results.

4.3 Discussions of the numerical results

For simplification of the consideration, we introduce the following notation for the critical radial stresses and critical compressive forces

$$\sigma_{cr}^{(1)}=\sigma_{rr.cr}^{(1),0}\Big/c_{44}^{(1)},\quad \sigma_{cr}^{(2)}=\sigma_{rr.cr}^{(2),0}\Big/c_{44}^{(1)},\quad \bar{p}_{cr}=p/c_{44}^{(1)} \tag{57}$$

Thus, according to (57), we estimate the work carrying capacity of the plate under consideration with respect to the buckling delamination by simultaneous use of the values of three dimensionless critical parameters which are the dimensionless radial compressive stress $\sigma_{cr}^{(1)}$ in the face piezoelectric layer, the dimensionless radial compressive stress $\sigma_{cr}^{(2)}$ in the core metal layer and the dimensionless intensity $\bar{p}_{cr}$ of the external compressive force. Such an approach for estimation of the buckling delamination allows us to have more precise information on the influence of the problem parameters such as the piezoelectricity of the face layers' materials, the face layers' thickness, the cracks' length (i.e., the radius of the penny-shaped cracks) and the mechanical properties of the layers' materials.

Thus, we consider the numerical results obtained for the critical parameters indicated in (57) and detailed above. Note that these results are given in Tables 4-9 which are obtained for the PZT-5H/Al/PZT-5H, PZT-4/Al/PZT-4, BaTiO3/Al/ BaTiO3, PZT-5H/St/PZT-5H, PZT-4/St/PZT-4 and BaTiO3/St/ BaTiO3 plates, respectively. For estimation of the influence of the face layers' piezoelectricity on the values of the critical stresses in the Tables, two types of results are presented simultaneously, the first of which (upper number) relates to the case where the values of the piezoelectric and dielectric constants of the face layer materials are equated to zero, i.e., coupling of the mechanical and electrical fields is not taken into consideration. However, under obtaining the second type of results (lower number) the values of the piezoelectric and dielectric constants are taken into consideration as given in Table 1 and the coupling effect between the electrical and mechanical fields is taken into consideration completely.

In these Tables the values of the critical stresses are also given for the same whole plate, i.e., the plate which does not contain any crack. These results are in the far right column and according to these results, the cases can be determined where the stability loss of the whole plate takes place in the early stage of external loading, before buckling delamination.

Thus, it follows from these Tables, and, as can be predicted, that the values of all the critical stresses related to the buckling delamination increase with increasing of the face-piezoelectric layers' thickness and with decreasing of the crack's radius. At the same time, these Tables show that in all the considered cases, the piezoelectricity of the face layers' materials causes an increase in the values of $\sigma_{cr}^{(1)}$, i.e. in the values of the critical compressive stress acting in the piezoelectric layer. According to the numerical results, we can also conclude that the influence of the piezoelectricity on the values of $\sigma_{cr}^{(2)}$, i.e. on the critical values of the compressive stress acting in the core-metal layer, is as follows: for the PZT-5H/Al/PZT-5H and PZT-5H/St?PZT-5H plates for all the considered cases, the piezoelectricity of the face layers' materials causes a decrease in the values of $\sigma_{cr}^{(2)}$, however for the PZT-4/Al/PZT-4, PZT-4/St/PZT-4, BaTiO3/Al/BaTiO3 and BaTiO3/St/BaTiO3 plates this conclusion occurs for the cases where $\ell_0/\ell\geq 0.2$.

Table 3 Comparison of the values $p_{cr}/E^{(1)}$ obtained by employing the present approach with the corresponding ones obtained in the paper by Rzayev and Akbarov (2002) for various values of $(\ell-\ell_0)/(2\ell)$ and h_F/ℓ under $2h_F/\ell_0=1/8$ and $E^{(2)}/E^{(1)}=50$: here h_F is a thickness of the face layer, ℓ_0 (ℓ) is a radius penny-shaped crack (plate-disc)

$\frac{\ell-\ell_0}{2\ell}$	$\frac{h_F}{\ell}$	The results obtained by the approach developed in the paper by Rzayev and Akbarov (2002); (FE numbers are 20 and 6 in the radial and thickness directions, respectively)	The results obtained by the approach developed in the present paper; (FE numbers are 40 and 12 in the radial and thickness directions, respectively)
0.10	0.0500	0.2571	0.2260
0.15	0.04375	0.2526	0.2343
0.20	0.0375	0.2509	0.2371
0.25	0.03125	0.2510	0.2380

Table 4 The values of the critical stresses $\sigma_{cr}^{(1)}$, $\sigma_{cr}^{(2)}$ and $\overline{p}_{cr}$ (57) obtained for PZT-5H/Al/PZT-5H in the cases where the piezoelectric constants of PZT are equated to zero (upper number), are different from zero, and are equal to the corresponding data given in Table 1 (lower number): here h_F is a thickness of the face layer, ℓ is a radius plate-disc

h_F/ℓ	Crit. Str.	ℓ_0/ℓ							
		0.70	0.60	0.50	0.40	0.30	0.20	0.10	0.00
0.025	$\sigma_{cr}^{(1)}$	0.0162	0.0217	0.0304	0.0454	0.0747	0.1418	0.3375	0.1404
		0.0236	0.0315	0.0440	0.0658	0.1082	0.2062	0.5012	0.1927
	$\sigma_{cr}^{(2)}$	0.0191	0.0255	0.0358	0.0535	0.0881	0.1906	0.3981	0.1656
		0.0161	0.0216	0.0301	0.0451	0.0742	0.1414	0.3438	0.1321
	$\overline{p}_{cr}$	0.0184	0.0246	0.0345	0.0516	0.0847	0.1609	0.3830	0.1593
		0.0180	0.0240	0.0337	0.0503	0.0827	0.1577	0.3832	0.1473
0.033	$\sigma_{cr}^{(1)}$	0.0277	0.0367	0.0508	0.0745	0.1183	0.2103	0.4347	0.1370
		0.0402	0.0532	0.0736	0.1080	0.1718	0.3081	0.6543	0.2017
	$\sigma_{cr}^{(2)}$	0.0326	0.0432	0.0599	0.0878	0.1395	0.2480	0.5127	0.1616
		0.0275	0.0364	0.0504	0.0740	0.1178	0.2113	0.4488	0.1383
	$\overline{p}_{cr}$	0.0310	0.0411	0.0569	0.0834	0.1324	0.2355	0.4867	0.1534
		0.0318	0.0421	0.0582	0.0853	0.1359	0.2436	0.5174	0.1595
0.042	$\sigma_{cr}^{(1)}$	0.0415	0.0545	0.0743	0.1068	0.1640	0.2751	0.5093	0.1341
		0.0602	0.0790	0.1078	0.1551	0.2393	0.4060	0.7752	0.2097
	$\sigma_{cr}^{(2)}$	0.0489	0.0642	0.0876	0.1259	0.1934	0.3245	0.6007	0.1581
		0.0412	0.0541	0.0739	0.1063	0.1641	0.2785	0.5317	0.1438
	$\overline{p}_{cr}$	0.0459	0.0602	0.0821	0.1179	0.1812	0.3039	0.5626	0.1481
		0.0492	0.0645	0.0881	0.1267	0.1954	0.3316	0.6332	0.1712
0.050	$\sigma_{cr}^{(1)}$	0.0571	0.0742	0.0999	0.1407	0.2094	0.3338	0.5669	0.1316
		0.0829	0.1077	0.1452	0.2050	0.3071	0.4965	0.8712	0.2169
	$\sigma_{cr}^{(2)}$	0.0673	0.0875	0.1178	0.1659	0.2470	0.3937	0.6687	0.1552
		0.0568	0.0738	0.0996	0.1406	0.2106	0.3406	0.5976	0.1487
	$\overline{p}_{cr}$	0.0623	0.0809	0.1089	0.1533	0.2282	0.3637	0.6178	0.1435
		0.0699	0.0908	0.1224	0.1728	0.2589	0.4186	0.7344	0.1829

In the cases where $\ell_0/\ell < 0.2$, for instance in the case where $\ell_0/\ell = 0.1$ the character of the influence of the piezoelectricity of the face layers depends on their thickness, i.e. under relatively thick face layers, for example under $h_F/\ell \geq 0.033$ for the BaTiO3/Al/BaTiO3 plate, the piezoelectricity causes an increase in the values of $\sigma_{cr}^{(2)}$.

Consider also the influence of the face layers' piezoelectricity on the values of $\overline{p}_{cr}$ for which, according to Tables 4 – 9, we can make the following conclusion: in general the character of the influence of the piezoelectricity on the values of $\overline{p}_{cr}$ depends on the values of h_F/ℓ and ℓ_0/ℓ, as well as on the selected materials of the layers. For instance, for the PZT-4/Al/PZT-4 and BaTiO3/Al/BaTiO3 plates for all the considered values of h_F/ℓ and ℓ_0/ℓ, the piezoelectricity of the face layer material causes an increase in the values of $\overline{p}_{cr}$, however, for the PZT-5H/Al/PZT-5H plate this increase takes place in the cases where $h_F/\ell \geq 0.042$. For the PZT-5H/St/PZT-5H, PZT-4/St/PZT-4 and BaTiO3/St/BaTiO3 plates in the cases where $\ell_0/\ell \leq 0.4$, the values of $\overline{p}_{cr}$ decrease as a result of the piezoelectricity under relatively thin face layers.

Thus, it follows from the foregoing discussions and from the numerical results given in Tables 4-8, that the most sensitive parameter for determination of the influence of the face layer piezoelectricity on the buckling delamination of the plate under consideration is the critical value of the radial compressive stress $\sigma_{cr}^{(1)}$ acting in the piezoelectric face layers.

Table 5 The values of the critical stresses $\sigma_{cr}^{(1)}$, $\sigma_{cr}^{(2)}$ and $\bar{p}_{cr}$ (57) obtained for PZT-4/Al/PZT-4 in the cases where the piezoelectric constants of PZT are equated to zero (upper number), are different from zero, and are equal to the corresponding data given in Table 1 (lower number): here h_F is a thickness of the face layer, ℓ is a radius plate-disc

h_F/ℓ	Crit. Str.	ℓ_0/ℓ							
		0.70	0.60	0.50	0.40	0.30	0.20	0.10	0.00
0.025	$\sigma_{cr}^{(1)}$	0.0199 0.0263	0.0265 0.0350	0.0369 0.0489	0.0548 0.0729	0.0890 0.1191	0.1650 0.2250	0.3733 0.5371	0.1572 0.1988
	$\sigma_{cr}^{(2)}$	0.0163 0.0146	0.0217 0.0194	0.0303 0.0271	0.0450 0.0404	0.0732 0.0661	0.1357 0.1249	0.3070 0.2982	0.1293 0.1103
	$\bar{p}_{cr}$	0.0172 0.0175	0.0230 0.0233	0.0320 0.0326	0.0475 0.0485	0.0771 0.0794	0.1430 0.1499	0.3236 0.3579	0.1363 0.1325
0.033	$\sigma_{cr}^{(1)}$	0.0338 0.0447	0.0445 0.0590	0.0611 0.0814	0.0887 0.1189	0.1387 0.1880	0.2400 0.3336	0.4717 0.6971	0.1613 0.2132
	$\sigma_{cr}^{(2)}$	0.0278 0.0248	0.0366 0.0327	0.0502 0.0451	0.0729 0.0660	0.1140 0.1043	0.1974 0.1852	0.3880 0.3870	0.1327 0.1183
	$\bar{p}_{cr}$	0.0298 0.0314	0.0392 0.0415	0.0539 0.0572	0.0782 0.0836	0.1223 0.1322	0.2116 0.2347	0.4159 0.4904	0.1423 0.1500
0.042	$\sigma_{cr}^{(1)}$	0.0502 0.0667	0.0655 0.0873	0.0886 0.1187	0.1257 0.1700	0.1896 0.2604	0.3088 0.4374	0.5455 0.8232	0.1649 0.2260
	$\sigma_{cr}^{(2)}$	0.0412 0.0370	0.0538 0.0484	0.0728 0.0659	0.1034 0.0943	0.1559 0.1445	0.2540 0.2428	0.4487 0.4570	0.1357 0.1255
	$\bar{p}_{cr}$	0.0450 0.0494	0.0587 0.0646	0.0794 0.0879	0.1127 0.1259	0.1700 0.1929	0.2768 0.3239	0.4891 0.6096	0.1480 0.1674
0.050	$\sigma_{cr}^{(1)}$	0.0686 0.0916	0.0885 0.1187	0.1180 0.1594	0.1638 0.2238	0.2390 0.3329	0.3696 0.5328	0.6018 0.9236	0.1680 0.2379
	$\sigma_{cr}^{(2)}$	0.0564 0.0508	0.0728 0.0659	0.0970 0.0885	0.1347 0.1242	0.1966 0.1848	0.3040 0.2958	0.4950 0.5128	0.1381 0.1320
	$\bar{p}_{cr}$	0.0625 0.0712	0.0806 0.0923	0.1075 0.1239	0.1492 0.1740	0.2178 0.2588	0.3368 0.4143	0.5484 0.7182	0.1531 0.1850

Table 6 The values of the critical stresses $\sigma_{cr}^{(1)}$, $\sigma_{cr}^{(2)}$ and $\bar{p}_{cr}$ (57) obtained for BaTiO3/Al/BaTiO3 in the cases where the piezoelectric constants of PZT are equated to zero (upper number), are different from zero, and are equal to the corresponding data given in Table 1 (lower number): here h_F is a thickness of the face layer, ℓ is a radius plate-disc

h_F/ℓ	Crit. Str.	ℓ_0/ℓ							
		0.70	0.60	0.50	0.40	0.30	0.20	0.10	0.00
0.025	$\sigma_{cr}^{(1)}$	0.0166 0.0178	0.0221 0.0238	0.0309 0.0331	0.0460 0.0494	0.0747 0.0806	0.1396 0.1511	0.3230 0.3553	0.1163 0.1238
	$\sigma_{cr}^{(2)}$	0.0099 0.0095	0.0131 0.0127	0.0183 0.0177	0.0273 0.0264	0.0444 0.0431	0.0829 0.0808	0.1917 0.1899	0.0690 0.0661
	$\bar{p}_{cr}$	0.0116 0.0116	0.0154 0.0155	0.0215 0.0216	0.0320 0.0322	0.0520 0.0525	0.0971 0.0984	0.2246 0.2313	0.0809 0.0806

Continued-

0.033	$\sigma_{cr}^{(1)}$	0.0282	0.0373	0.0512	0.0746	0.1172	0.2049	0.4135	0.1245
		0.0303	0.0400	0.0552	0.0804	0.1267	0.2231	0.4584	0.1339
	$\sigma_{cr}^{(2)}$	0.0167	0.0221	0.0304	0.0442	0.0696	0.1216	0.2454	0.0739
		0.0161	0.0213	0.0295	0.0430	0.0677	0.1192	0.2450	0.0716
	$\overline{p}_{cr}$	0.0206	0.0272	0.0374	0.0544	0.0855	0.1494	0.3015	0.0908
		0.0209	0.0276	0.0381	0.0555	0.0874	0.1539	0.3161	0.0924
0.042	$\sigma_{cr}^{(1)}$	0.0422	0.0550	0.0745	0.1061	0.1610	0.2658	0.4833	0.1318
		0.0453	0.0591	0.0803	0.1146	0.1748	0.2911	0.5391	0.1429
	$\sigma_{cr}^{(2)}$	0.0250	0.0326	0.0442	0.0630	0.0956	0.1577	0.2869	0.0782
		0.0242	0.0316	0.0429	0.0612	0.0934	0.1556	0.2881	0.0763
	$\overline{p}_{cr}$	0.0322	0.0420	0.0569	0.0810	0.1229	0.2028	0.3688	0.1006
		0.0330	0.0431	0.0585	0.0835	0.1274	0.2121	0.3927	0.1041
0.050	$\sigma_{cr}^{(1)}$	0.0577	0.0745	0.0996	0.1389	0.2044	0.3208	0.5382	0.1385
		0.0620	0.0802	0.1076	0.1505	0.2227	0.3532	0.6033	0.1511
	$\sigma_{cr}^{(2)}$	0.0342	0.0442	0.0591	0.0824	0.1213	0.1905	0.3195	0.0822
		0.0331	0.0429	0.0575	0.0804	0.1190	0.1887	0.3224	0.0808
	$\overline{p}_{cr}$	0.0460	0.0594	0.0794	0.1107	0.1629	0.2557	0.4289	0.1104
		0.0476	0.0616	0.0826	0.1155	0.1709	0.2710	0.4629	0.1160

Table 7 The values of the critical stresses $\sigma_{cr}^{(1)}$, $\sigma_{cr}^{(2)}$ and $\overline{p}_{cr}$ (57) obtained for PZT-4/St/PZT-4 in the cases where the piezoelectric constants of PZT are equated to zero (upper number), are different from zero, and are equal to the corresponding data given in Table 1 (lower number): here h_F is a thickness of the face layer, ℓ is a radius plate-disc

h_F/ℓ	Crit. Str.	ℓ_0/ℓ							
		0.70	0.60	0.50	0.40	0.30	0.20	0.10	0.00
0.025	$\sigma_{cr}^{(1)}$	0.0164	0.0220	0.0309	0.0465	0.0769	0.1473	0.3554	0.1130
		0.0239	0.0321	0.0450	0.0677	0.1121	0.2164	0.5365	0.1527
	$\sigma_{cr}^{(2)}$	0.0256	0.0705	0.0990	0.1486	0.2458	0.4708	1.1361	0.3612
		0.0445	0.0596	0.0837	0.1259	0.2084	0.4022	0.9972	0.2838
	$\overline{p}_{cr}$	0.0436	0.0584	0.0820	0.1231	0.2036	0.3900	0.9410	0.2992
		0.0394	0.0528	0.0741	0.1114	0.1844	0.3558	0.8821	0.2511
0.033	$\sigma_{cr}^{(1)}$	0.0282	0.0374	0.0520	0.0766	0.1224	0.2198	0.4585	0.0918
		0.0411	0.0546	0.0758	0.1118	0.1795	0.3258	0.7038	0.1365
	$\sigma_{cr}^{(2)}$	0.0902	0.1198	0.1664	0.2448	0.3914	0.7024	1.4654	0.2935
		0.0764	0.1015	0.1410	0.2079	0.3336	0.6056	1.3082	0.2537
	$\overline{p}_{cr}$	0.0696	0.0924	0.1283	0.1888	0.3018	0.5416	1.1298	0.2263
		0.0647	0.0859	0.1193	0.1759	0.2823	0.5124	1.1068	0.2147
0.042	$\sigma_{cr}^{(1)}$	0.0424	0.0558	0.0764	0.1103	0.1706	0.2884	0.5368	0.0758
		0.0618	0.0814	0.1116	0.1616	0.2515	0.4318	0.8353	0.1236
	$\sigma_{cr}^{(2)}$	0.1356	0.1785	0.2445	0.3526	0.5453	0.9219	1.7157	0.2425
		0.1149	0.1513	0.2075	0.3004	0.4674	0.8025	1.5526	0.2298
	$\overline{p}_{cr}$	0.0968	0.1274	0.1745	0.2519	0.3892	0.6580	1.2245	0.1731
		0.0928	0.1222	0.1676	0.2426	0.3775	0.6481	1.2538	0.1855

Continued-

0.050	$\sigma_{cr}^{(1)}$	0.0585	0.0763	0.1032	0.1459	0.2186	0.3506	0.5963	0.0640
		0.0854	0.1115	0.1511	0.2146	0.3243	0.5297	0.9381	0.1133
	$\sigma_{cr}^{(2)}$	0.1872	0.2440	0.3299	0.4666	0.6987	1.1205	1.9060	0.2045
		0.1587	0.2072	0.2808	0.3989	0.6028	0.9846	1.7436	0.2106
	$\bar{p}_{cr}$	0.1229	0.1602	0.2166	0.3063	0.4587	0.7356	1.2512	0.1343
		0.1221	0.1594	0.2160	0.3068	0.4636	0.7572	1.3409	0.1620

Table 8 The values of the critical stresses $\sigma_{cr}^{(1)}$, $\sigma_{cr}^{(2)}$ and $\bar{p}_{cr}$ (57) obtained for PZT-5H/St/PZT-5H in the cases where the piezoelectric constants of PZT are equated to zero (upper number), are different from zero, and are equal to the corresponding data given in Table 1 (lower number): here h_F is a thickness of the face layer, ℓ is a radius plate-disc

h_F/ℓ	Crit. Str.	ℓ_0/ℓ							
		0.70	0.60	0.50	0.40	0.30	0.20	0.10	0.00
0.025	$\sigma_{cr}^{(1)}$	0.0202	0.0270	0.0377	0.0563	0.0920	0.1722	0.3939	0.2326
		0.0267	0.0358	0.0502	0.0752	0.1239	0.2373	0.5788	0.2892
	$\sigma_{cr}^{(2)}$	0.0451	0.0601	0.0842	0.1254	0.2050	0.3837	0.8780	0.5184
		0.0402	0.0539	0.0755	0.1131	0.1865	0.3570	0.8707	0.4350
	$\bar{p}_{cr}$	0.0389	0.0519	0.0726	0.1082	0.1768	0.3309	0.7570	0.1793
		0.0369	0.0494	0.0692	0.1037	0.1709	0.3270	0.7978	0.1599
0.033	$\sigma_{cr}^{(1)}$	0.0344	0.0455	0.0628	0.0916	0.1442	0.2517	0.4975	0.2016
		0.0457	0.0607	0.0841	0.1236	0.1973	0.3549	0.7553	0.2681
	$\sigma_{cr}^{(2)}$	0.0768	0.1015	0.1401	0.2043	0.3216	0.5611	1.1088	0.4494
		0.0689	0.0914	0.1265	0.1859	0.2968	0.5339	1.1362	0.4033
	$\bar{p}_{cr}$	0.0627	0.0829	0.1144	0.1668	0.2625	0.4580	0.9050	0.1373
		0.0612	0.0812	0.1124	0.1652	0.2637	0.4743	1.0093	0.1340
0.042	$\sigma_{cr}^{(1)}$	0.0514	0.0673	0.0915	0.1305	0.1981	0.3247	0.5739	0.1769
		0.0686	0.0902	0.1234	0.1779	0.2752	0.4680	0.8937	0.2504
	$\sigma_{cr}^{(2)}$	0.1147	0.1500	0.2039	0.2909	0.4415	0.7238	1.2791	0.3942
		0.1033	0.1357	0.1857	0.2676	0.4140	0.7040	1.3445	0.3767
	$\bar{p}_{cr}$	0.0884	0.1156	0.1571	0.2241	0.3401	0.5576	0.9853	0.1055
		0.0889	0.1168	0.1598	0.2303	0.3562	0.6057	1.1567	0.1126
0.050	$\sigma_{cr}^{(1)}$	0.0705	0.0913	0.1223	0.1707	0.2505	0.3891	0.6310	0.1573
		0.0947	0.1233	0.1665	0.2354	0.3534	0.5720	1.0022	0.2359
	$\sigma_{cr}^{(2)}$	0.1572	0.2036	0.2726	0.3804	0.5582	0.8674	1.4065	0.3506
		0.1424	0.1854	0.2504	0.3541	0.5317	0.8605	1.5077	0.3550
	$\bar{p}_{cr}$	0.1139	0.1475	0.1975	0.2756	0.4044	0.6283	1.0188	0.0814
		0.1186	0.1544	0.2085	0.2948	0.4426	0.7163	1.2550	0.0947

Comparison of the numerical results given in Tables 4, 5 and 6 with the corresponding ones given in Tables 7, 8 and 9, respectively, shows that the values of the critical stresses obtained for the plates with the St-core layer are greater than those obtained for the plates with the Al-core layer.

This comparison also shows that the values of $\sigma_{cr}^{(1)}$ depend mainly on the geometrical and electro-mechanical properties of the face layer material, however the values of $\sigma_{cr}^{(2)}$ and $\bar{p}_{cr}$ depend mainly on the geometrical and mechanical properties of the core layer material.

Table 9 The values of the critical stresses $\sigma_{cr}^{(1)}$, $\sigma_{cr}^{(2)}$ and $\bar{p}_{cr}$ (57) obtained for BaTiO3/St/BaTiO3 in the cases where the piezoelectric constants of PZT are equated to zero (upper number), are different from zero, and are equal to the corresponding data given in Table 1 (lower number): here h_F is a thickness of the face layer, ℓ is a radius plate-disc

h_F/ℓ	Crit. Str.	ℓ_0/ℓ							
		0.70	0.60	0.50	0.40	0.30	0.20	0.10	0.00
0.025	$\sigma_{cr}^{(1)}$	0.0170	0.0227	0.0318	0.0475	0.0781	0.1477	0.3482	0.1685
		0.0182	0.0244	0.0342	0.0511	0.0842	0.1603	0.3856	0.1787
	$\sigma_{cr}^{(2)}$	0.0273	0.0365	0.0512	0.0765	0.1256	0.2375	0.5600	0.2711
		0.0264	0.0353	0.0495	0.0741	0.1220	0.2322	0.5585	0.2588
	$\bar{p}_{cr}$	0.0248	0.0331	0.0464	0.0693	0.1138	0.2151	0.5071	0.0627
		0.0244	0.0326	0.0457	0.0684	0.1126	0.2143	0.5153	0.0610
0.033	$\sigma_{cr}^{(1)}$	0.0290	0.0384	0.0532	0.0779	0.1233	0.2184	0.4469	0.1555
		0.0312	0.0414	0.0572	0.0840	0.1337	0.2388	0.5001	0.1676
	$\sigma_{cr}^{(2)}$	0.0468	0.0619	0.0855	0.1254	0.1984	0.3512	0.7188	0.2501
		0.0452	0.0599	0.0829	0.1217	0.1936	0.3458	0.7241	0.2428
	$\bar{p}_{cr}$	0.0409	0.0541	0.0748	0.1095	0.1734	0.3070	0.6282	0.0535
		0.0406	0.0538	0.0744	0.1092	0.1737	0.3102	0.6495	0.0533
0.042	$\sigma_{cr}^{(1)}$	0.0435	0.0570	0.0777	0.1114	0.1707	0.2847	0.5223	0.1447
		0.0467	0.0614	0.0838	0.1206	0.1858	0.3134	0.5891	0.1585
	$\sigma_{cr}^{(2)}$	0.0700	0.0917	0.1251	0.1792	0.2745	0.4579	0.8401	0.2328
		0.0677	0.0889	0.1214	0.1747	0.2690	0.4539	0.8530	0.2295
	$\bar{p}_{cr}$	0.0590	0.0773	0.1054	0.1510	0.2313	0.3858	0.7077	0.0459
		0.0600	0.0775	0.1058	0.1522	0.2344	0.3954	0.7431	0.0468
0.050	$\sigma_{cr}^{(1)}$	0.0598	0.0776	0.1043	0.1466	0.2174	0.3444	0.5803	0.1356
		0.0644	0.0838	0.1129	0.1592	0.2379	0.3816	0.6588	0.1507
	$\sigma_{cr}^{(2)}$	0.0961	0.1249	0.1678	0.2357	0.3497	0.5541	0.9334	0.2181
		0.0933	0.1213	0.1636	0.2305	0.3444	0.5525	0.9539	0.2182
	$\bar{p}_{cr}$	0.0780	0.1013	0.1361	0.1912	0.2836	0.4493	0.7569	0.0395
		0.0789	0.1026	0.1383	0.1949	0.2912	0.4671	0.8064	0.0412

5. Conclusions

Thus, in the present paper within the scope of the three-dimensional linearized theory of stability for piezoelectric materials, the axisymmetric buckling delamination of the PZT/Metal/PZT sandwich circular plate with interface penny-shaped cracks has been investigated. The case where open-circuit conditions with respect to the electrical displacement on the upper and lower surfaces, and short-circuit conditions with respect to the electrical potential on the lateral surface of the face layers are satisfied, is considered. It is assumed that the edge surfaces of the cracks have an infinitesimal rotationally symmetric initial imperfection and the development of this imperfection is studied by employing the exact geometrically non-linear field equations and relations of electro-elasticity for piezoelectric materials. The sought values are presented in the power series form with respect to the small parameter which characterizes the degree of the initial imperfection. By use of the corresponding mathematical manipulations, the corresponding equations and relations are obtained for the zeroth and first approximations which are enough for investigating the stability loss and buckling delamination problems. It is established that the equations and relations related to the first approximation coincide with the corresponding ones of the three-dimensional-linearized theory of electro-elasticity for the piezoelectric materials. The quantities related to the zeroth approximation are determined analytically, however, the quantities related to the first approximation are determined numerically by employing FEM. For determination of the critical values of the compressive stresses, the initial imperfection criterion is used. Numerical results are presented in Tables 4 – 9 for the PZT-5H/Al/PZT-5H, PZT-4/Al/PZT-4, BaTiO3/Al/ BaTiO3, PZT-5H/St/PZT-5H, PZT-4/St/PZT-4 and BaTiO3/St/ BaTiO3 plates, respectively. These results illustrate simultaneously the values of the critical

dimensionless radial compressive stress $\sigma_{cr}^{(1)}$ acting in the face piezoelectric layer, the values of the dimensionless critical compressive radial stress $\sigma_{cr}^{(2)}$ acting in the core-metal layer and the values of the dimensionless critical stress of the intensity $\overline{p}_{cr}$ of the external compressive forces obtained in the case where the piezoelectricity, i.e., the coupling effect, are taken into consideration (lower number in the Tables) and in the case where the coupling effect is not taken into consideration (upper number in the Tables). According to these results, the following concrete conclusions can be drawn:

- The values of $\sigma_{cr}^{(1)}$, $\sigma_{cr}^{(2)}$ and $\overline{p}_{cr}$ decrease with decreasing of the face layer thickness and with increasing of the crack's radius;
- For all the considered concrete cases, the piezoelectricity of the face layer material causes an increase in the values of $\sigma_{cr}^{(1)}$ and this increase becomes more considerable with face layer thickness;
- The character of the influence of the face layers' materials' piezoelectricity on the values of $\sigma_{cr}^{(2)}$ and $\overline{p}_{cr}$ depends on the electro-mechanical and geometrical characteristics of the constituents of the plate: as a rule, for relatively thin (thick) face layers and for relatively long (short) cracks, as a result of the piezoelectricity, the values of $\sigma_{cr}^{(2)}$ and $\overline{p}_{cr}$ decrease (increase). However, the magnitude of these "increases" and "decreases" is significantly less than that obtained for $\sigma_{cr}^{(1)}$;
- The values of $\sigma_{cr}^{(1)}$, $\sigma_{cr}^{(2)}$ and $\overline{p}_{cr}$ obtained for the plates with St-core layer are greater than the corresponding ones obtained for the plates with Al-core layer;
- The values of $\sigma_{cr}^{(1)}$ play a dominant role in the geometrical and electro-mechanical characteristics of the face layer, however, the values of $\sigma_{cr}^{(2)}$ and $\overline{p}_{cr}$ play a dominant role in the geometrical and mechanical characteristics of the core layer material;
- The most sensitive parameter for determination of the influence of the face layer piezoelectricity on the buckling delamination of the plate under consideration, is $\sigma_{cr}^{(1)}$.

References

Akbarov, S.D. (2013), *Stability Loss and Buckling Delamination: Three-Dimensional Linearized Approach for Elastic and Viscoelastic Composites*. Springer, Heidelberg, New York.

Akbarov, S.D. and Rzayev, O.G. (2002), "On the buckling of the elastic and viscoelastic composite circular thick plate with a penny-shaped crack", *Eur. J Mech. A Solid*. **21**(2), 269 -279.

Akbarov, S.D. and Yahnioglu, N. (2013), "Buckling delamination of a sandwich plate-strip with piezoelectric face and elastic core layers", *Appl. Math. Model*. **37**, 8029-8038

Akbarov, S.D. and Yahnioglu, N. (2016), "On the total electro-mechanical potential energy and energy release rate at the interface crack tips in an initially stressed sandwich plate-strip with , piezoelectric face and elastic core layers", *Int. J. Solid Struct*., **88-89**, 119-130

Arefi, M. and Allam, M.N.M. (2015), "Nonlinear responses of an arbitrary FGP circular plate resting on the

Bogdanov, V.L., Guz, A.N. and Nazarenko V.M. (2015), "Spatial problems of the fracture of materials loaded along cracks (Review)", *Int. Appl. Mech*., **51**(5), 489-560.

Guz, A.N. (1999), *Fundamentals of the Three-Dimensional Theory of Stability of Deformable Bodies*. Springer -Verlag, Berlin Heidelberg.

Guz, A.N. (2004), *Elastic waves in bodies with initial (residual) stresses*. "A.C.K.", Kiev.

Guz, A.N. and Nazarenko, V.M. (1985), "Symmetric failure of the half-space with penny-shaped crack in compression", *Theor. Appl. Fcat. Mec.*, **3**, 233-245.

Jabbari, M., Farzaneh Joubaneh, E., Khorshidvand, A.R. and Eslami, M.R. (2013), "Buckling analysis of porous circular plate with piezoelectric actuator layers under uniform radial compression", *Int. J. Mech. Sci*., **70**, 50-56.

Jerome, R. and Ganesan, N. (2010). "New generalized plane strain FE formulation for the buckling analysis of piezocomposite beam", *Finit. Elem. Anal. Des.*, **46**, 896-904.

Kakar, R. and Kakar, S. (2016), "SH-waves in a piezoelectric layer overlying an initially stressed orthotropic half- space", *Smart Struct. Syst.*, 17 (2), 327-345.

Kuna, M. (2006), "Finite element analysis of cracks in piezoelectric structures: a survey", *Arch. Appl. Mech*., **76**, 725-745.

Meng, F., Wang H., Wang, X. and Li, Z. (2010), "Elliptically delaminated buckling near the surface of piezoelectric laminated shells under electric and thermal loads", *Compos. Struct.*, **92**(3), 684-690

Rzayev, O.G. and Akbarov, S.D. (2002), "Local buckling of the elastic and viscoelastic coating around the penny- shaped interface crack", *Int. J Eng. Sci*., **40**, 1435-1451.

Winkler – Pasternak foundation", *Smart Struct. Syst.*, **16**(1), 81-100.

Wu, C.P. and Ding, S. (2015), "Coupled electro-elastic analysis of functionally graded piezoelectric material plates", *Smart Struct. Syst.*, **16**(5), 781-806.

Yang, J.S. (1998), "Buckling of a piezoelectric plate", *Int. J. Appl. Electromagn. Mech*., **9**, 399-408.

Yang, J.S. (2005), An introduction to the theory of piezoelectricity. Springer, New-York.

Zienkiewicz, O.C. and Taylor, R.L. (1989), *Basic formulation and linear problems. The finite element method*, **1**, 4-th Ed., McGraw-Hill, New York.

CC